

Nanoscale Heterostructures with Molecular-Scale Single-Crystal Metal Wires

Paromita Kundu,[†] Aditi Halder,[†] B. Viswanath,[†] Dipan Kundu,[†] Ganpati Ramanath,[‡] and N. Ravishankar^{*,†}

Materials Research Centre, Indian Institute of Science, Bangalore 560 012, India, and Materials Science and Engineering Department, Rensselaer Polytechnic Institute, Troy, New York 12180

Received September 22, 2009; E-mail: nravi@mrc.iisc.ernet.in

Nanoscale heterostructures with engineered metal-semiconductor interfaces are potential candidates for a variety of applications including field-effect transistors,¹ photodetectors, photodiodes,² solar cells,³ catalysis,⁴ nanodevice wiring,⁵ and sensing. Several methods exist to attach equiaxed metal nanoparticles to substrates. However, anchoring *molecular-scale* (<2-nm-diameter) single-crystal metal wires to other materials and substrates is yet to be realized because it is only recently that nanowires with such small dimensions have been synthesized.^{6,7} Here, we demonstrate a simple wet-chemical approach for site-selectively nucleating and growing molecular-scale single-crystal gold wires from nanostructure substrates of different materials.

We recently showed that Au(III) reduction to metallic Au wires by amine in toluene proceeds via rocksalt AuCl nanocube formation.^{8,9} Here, we reduce the AuCl nanocubes on nanostructure substrate surfaces to Au nanoparticles, which serve as seeds for single-crystal nanowire growth from solution phase flux through an oriented attachment mechanism.⁶ This method is general and applicable to fabricating single-crystal Au nanowires from a variety of materials including ZnO nanorods, MgO nanocubes, carbon nanotubes (CNTs), and hydroxyapatite nanorods. This site-specific attachment approach can serve as a new paradigm for synthesizing anisotropic nanoscale heterostructures with molecular-scale single-crystal metal nanowires for applications.

Figure 1a shows a schematic illustration of our approach. We first nucleate AuCl on the desired substrates by reducing chloroauric acid with oleylamine. Experiments on nanostructure substrates with different structural and bonding characteristics show that heterogeneous nucleation of AuCl on the nanostructure substrates is preferred over homogeneous nucleation for all substrates explored except CNTs, which require an acid pretreatment for heterogeneous nucleation.

Bright-field transmission electron microscopy (TEM) shows rocksalt AuCl cubes connected with ZnO nanorod (Figure 1b) and CNT (Figure 1c) substrate surfaces even after vigorous washing and drying. Analysis of several micrographs shows that the AuCl crystal size ranges from 30 to 70 nm with an average of ~50 nm. X-ray diffractograms from heterostructures synthesized with MgO nanocubes (Figure 1d) or ZnO nanorods (Figure S1, Supporting Information) showing the (200) reflection are consistent with the rocksalt AuCl structure reported recently.⁸ Core-level Au 4f bands and the Cl 2p band acquired by X-ray photoelectron spectroscopy indicate the presence of Au(I) and chloride species, further confirming that the cubes do indeed correspond to AuCl (Figure S2, Supporting Information). The presence of Au(0) is indicative of metal nanostructure formation by AuCl decomposition as described recently.⁸

The AuCl cubes are unstable under the electron beam and fragment into Au nanoparticles by reduction (Figure S3, Supporting

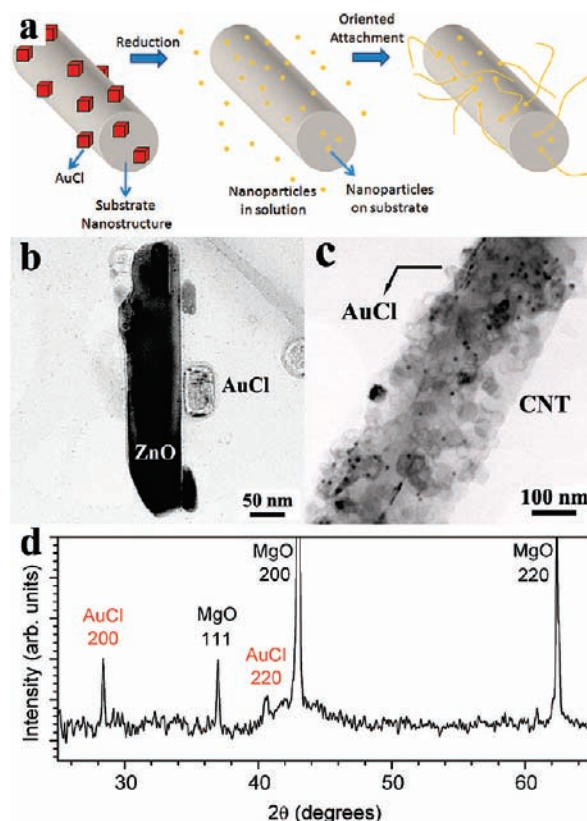


Figure 1. (a) Schematic illustration of the steps involved in the nucleation and growth of molecular scale wires from a cylindrical nanostructure substrate. Bright-field TEM images showing AuCl nanocubes nucleated on (b) ZnO nanorod and (c) CNT surfaces. (d) X-ray diffractogram showing AuCl formation on MgO nanocubes.

Information). Room temperature aging of the solution containing the cubes also leads to amine-capped ultrafine (~2 nm or less in diameter) Au nanoparticles that are present both in the solution and attached to the substrate (Figure S4, Supporting Information). Addition of ascorbic acid causes removal of the amine capping agent from the {111} facets of the attached particles, thus serving as anchor points from which the molecular-scale single-crystal metal nanowires (see Supporting Information Figure S5) grow by the oriented attachment mechanism.⁶ The mechanism is similar to the growth of wires by collision of particles in the solution phase. Here, the particle attached to the substrate serves as the origin for wire formation leading to the formation of nanoscale heterostructures.

Figure 2a–e show representative bright-field TEM images of the molecular scale Au nanowires grown from different nanostructures. The wire diameter is <2 nm, and the length varies from a few 100 nm to a few micrometers. In all these cases, the nanowires originate from and/or terminate on nanostructure substrates, apparent

[†] Indian Institute of Science.
[‡] Rensselaer Polytechnic Institute.

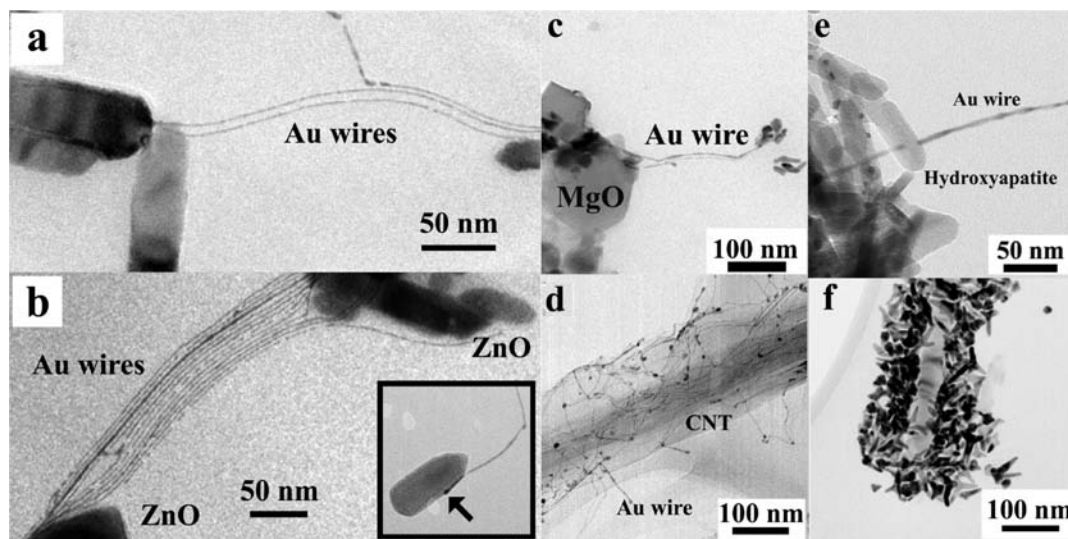


Figure 2. Bright field TEM images of molecular scale Au nanowires (a) originating from and (b) terminating at ZnO nanorods, on (c) MgO nanocube, (d) carbon nanotube, and (e) hydroxyapatite nanorod. (f) multipodal Au nanostructures grown on ZnO nanorod surfaces.

from one end of the nanowire being always attached to the nanostructure substrates. In many instances, the wires bridge a connection between the substrate nanostructures; e.g., see Figure 2a, b. Typically, the Au nanoparticle seeds on the substrate nanostructures have a slightly larger diameter compared to that of the nanowires that emanate from them (inset Figure 2b). This observation suggests that while the Au nanoparticle seeds form by AuCl reduction on the substrate through heterogeneous nucleation, the Au nanoparticles that attach onto the seed are those formed by homogeneous nucleation in the solution. Another possibility for the size difference is that incomplete reduction of AuCl allows only a part of it to transform to Au, which can seed nanowire growth. Prolonged physical mixing of the substrate nanostructures in solutions containing the AuCl cubes or ultrafine Au nanoparticles does not show nanowires emerging from nanostructure substrates, ruling out the possibility of junction formation due to aggregation in solution or drying (Supporting Information Figure S6). This result suggests that AuCl nucleation on the substrate surface is a key step that enables the formation of the heterostructure junctions.

The areal density of the molecular scale single-crystal nanowires formed on the nanostructure substrates correlates well with the number density of the AuCl cubes nucleated on the surface. For example, we observe only one or two AuCl cubes on each ZnO nanorod substrate (Figure 1b), typically leading to a small, discrete number of regions from which the nanowires originate on the surface (Figure 2a, b). Such an observation is also seen in the case of MgO cubes and hydroxyapatite nanorods (Figure 2c, e). In contrast, we find several tens of AuCl cubes distributed over $\sim 0.6\text{-}\mu\text{m}$ -long CNT surfaces (Figure 1d), leading to the origination of a much higher number of wires emanating from multiple points on the CNT surface (Figure 2d).

Figure 2f illustrates that attachment of multipodal structures of Au on the surface of a ZnO nanorod. The multipodal structures form by a low temperature process (at 273 K) through ascorbic acid reduction of Au ions on pre-existing particles formed on the surface (see Supporting Information). This result shows that our method of heterogeneous nucleation of the intermediate AuCl phase can conceivably be extended to other types of anisotropic nanostructures.

In conclusion, we have demonstrated a simple wet-chemical method to grow molecular scale wires from different nanostructure substrates. The nucleation of Au nanostructure seeds through the formation and

reduction of an intermediate AuCl phase on the substrate is a key step, which is followed by oriented attachment of Au nanoparticles formed in solution. Since nanostructured intermediates are known to form in Pt¹⁰ and Pd also, our method could be conceivably adapted to synthesize single-crystal wires of these noble metals. Finally, our method opens up, for the first time, the possibility to produce nanoscale heterostructure architectures with molecular scale metal nanowires that could be attractive for diverse applications in nanoelectronic device wiring, catalysis, and sensing.

Acknowledgment. N.R. thanks the Nanoscience and Technology Initiative (NSTI), Department of Science and Technology (DST) for financial support. G.R. acknowledges support from the US NSF and the NRI-NIST index grants.

Supporting Information Available: Synthesis conditions; characterization techniques; XRD, XPS, TEM analysis of the nanoscale heterostructures. This material is available free of charge via the Internet at <http://pubs.acs.org>.

References

- (1) Yoshida, S.; Suzuki, J. *J. Appl. Phys.* **1998**, *84* (5), 2940–2942. Wu, Y.; Xiang, J.; Yang, C.; Lu, W.; Lieber, C. M. *Nature* **2004**, *430* (6995), 61–65.
- (2) Endo, H.; Sugibuchi, M.; Takahashi, K.; Goto, S.; Sugimura, S.; Hane, K.; Kashiwaba, Y. *Appl. Phys. Lett.* **2007**, *90* (12), 121906–3.
- (3) Chandrasekharan, N.; Kamat, P. V. *J. Phys. Chem. B* **2000**, *104* (46), 10851–10857. Nakato, Y.; Ueda, K.; Yano, H.; Tsubomura, H. *J. Phys. Chem.* **2002**, *92* (8), 2316–2324.
- (4) Valden, M.; Lai, X.; Goodman, D. W. *Science* **1998**, *281*. Subramanian, V.; Wolf, E. E.; Kamat, P. V. *J. Am. Chem. Soc.* **2004**, *126* (15), 4943–4950. Hirakawa, T.; Kamat, P. V. *J. Am. Chem. Soc.* **2005**, *127* (11), 3928–3934.
- (5) Lu, W.; Lieber, C. M. *Nat. Mater.* **2007**, *6*, 841–850. McAlpine, M. C.; Ahmad, H.; Wang, D.; Heath, J. R. *Nat. Mater.* **2007**, *6*, 379–384. Cui, Y.; Wei, Q.; Park, H.; Lieber, C. M. *Science* **2001**, *293*, 1288–1292.
- (6) Halder, A.; Ravishankar, N. *Adv. Mater.* **2007**, *19* (14), 1854–1858.
- (7) Lu, X.; Yavuz, M. S.; Tuan, H.-Y.; Korgel, B. A.; Xia, Y. *J. Am. Chem. Soc.* **2008**, *130* (28), 8900–8901. Pazos-Perez, N.; Baranov, D.; Irsen, S.; Hilgendorff, M.; Liz-Marzan, L. M.; Giersig, M. *Langmuir* **2008**, *24* (17), 9855–9860. Huo, Z.; Tsung, C.-k.; Huang, W.; Zhang, X.; Yang, P. *Nano Lett.* **2008**, *8* (7), 2041–2044. Wang, C.; Sun, S. *Chem.—Asian J.* **2009**, *4*, 1028–1034.
- (8) Halder, A.; Kundu, P.; Ravishankar, N.; Ramanath, G. *J. Phys. Chem. C* **2009**, *113* (14), 5349–5351.
- (9) Halder, A.; Ravishankar, N. *J. Phys. Chem. B* **2006**, *110* (13), 6595–6600.
- (10) Halder, A.; Sharma, S.; Hegde, M. S.; Ravishankar, N. *J. Phys. Chem. C* **2009**, *113* (4), 1466–1473.

JA907874H